Colloids and Surfaces B: Biointerfaces 217 (2022) 112617

Contents lists available at ScienceDirect

Colloids and Surfaces B: Biointerfaces

journal homepage: www.elsevier.com/locate/colsurfb

Adsorption of flexible proteins in the 'wrong side' of the isoelectric point: Casein macropeptide as a model system

Pablo M. Blanco [a,d], Micaela M. Achetoni [b], Josep L. Garcés [c], Sergio Madurga [d], Francesc Mas [d], María F. Baieli [e], Claudio F. Narambuena [b,*]

[a] Department of Physical and Macromolecular Chemistry, Faculty of Science, Charles University, Hlavova 8, 128 00 Prague 2, Czech Republic
[b] Universidad Tecnología Nacional & Grupo Bionanotecnología y Sistemas Complejos. (UTN-CONICET), Facultad Regional San Rafael, Av. General Urquiza 314C. P.:5600, San Rafael, Mendoza, Argentina
[c] Department of Chemistry, University of Lleida, Av. Alcalde Rovira Roure 191, E-25198 Lleida, Catalonia, Spain
[d] Department of Material Science and Physical Chemistry & Institute of Theoretical and Computational Chemistry (IQTC), University of Barcelona, C/ Martí i Franquès, 1, 08028 Barcelona, Catalonia, Spain
[e] Universidad de Buenos Aires & Instituto de Nanobiotecnología (UBA-CONICET), Facultad de Farmacia y Bioquímica, Buenos Aires, Argentina

ARTICLE INFO

Keywords:
Casein macropeptide
Casein glycomacropeptide
Peptide adsorption
Adsorption on the wrong side of the isoelectric point
Charge regulation
Monte Carlo simulation
Constant pH simulation
Charge patches

ABSTRACT

We analyze the conditions of the adsorption of a flexible peptide onto a charged substrate in the 'wrong side' of the isoelectric point (WSIP), i.e. when surface and peptide charges have the same sign. As a model system, we focus on the casein macropeptide (CMP), both in the aglycosylated (aCMP) and fully glycosydated (gCMP) forms. We model the substrate as a uniformly charged plane while CMP is treated as a bead-and-spring model including electrostatic interactions, excluded volume effects and acid/base equilibria. Adsorption coverage, aminoacid charges and concentration profiles are computed by means of Monte Carlo simulations at fixed pH and salt concentration. We conclude that for different reasons the CMP can be adsorbed to both positively and negatively charged surfaces in the WSIP. For negatively charged surfaces, WSIP adsorption is due to the patchy distribution of charges: the peptide is attached to the surface by the positively charged end of the chain, while the repulsion of the surface for the negatively charged tail is screened by the small ions of the added salt. This effect increases with salt concentration. Conversely, a positively charged substrate induces strong charge regulation of the peptide: the acidic groups are deprotonated, and the peptide becomes negatively charged. This effect is stronger at low salt concentrations and it is more intense for gCMP than for aCMP, due to the presence of the additional sialic groups in gCMP.

1. Introduction

Protein adsorption to charged macromolecules, nanoparticles or surfaces usually involves the interplay of many different physicochemical phenomena, which sometimes lead to surprising or counter-intuitive behaviors [1]. A paradigmatic example is the attractive interaction between a charged substrate and a protein molecule when the sign of their net charges is the same [2–5]. Since such attractive interaction is not intuitively expected on these conditions, it is often described as complexation/adsorption in the wrong side of the isoelectric point (WSIP) [6].

Two hypotheses are found in the literature to explain this phenomenon. The first one is based on the presence of charge patches on the protein surface with charge sign opposite to that of the protein global charge [2,3,5,7–11]. In this way, the protein can overcome the electrostatic repulsion and remain attached to the surface. The second mechanism builds on the ability of the protein to modulate its charge in response to external perturbations (e.g., an electric field caused by an object with a large net charge) through the acid/base equilibrium, which is known as charge regulation [12]. Kirkwood had already predicted [12] that charge fluctuations resulting from charge regulation could produce attraction between two proteins with the same charge sign. This fact has also been confirmed by other authors [13]. If the electric field produced by a charged surface is strong enough, charge regulation could produce the inversion of the protein charge sign, thus inducing its complexation/adsorption on the WSIP [6,14–16]. This

* Correspondence to: Facultad Regional San Rafael, Universidad Tecnológica Nacional, San Rafael, Mendoza. Argentina.
E-mail address: claudionarambuena@gmail.com (C.F. Narambuena).

https://doi.org/10.1016/j.colsurfb.2022.112617
Received 27 December 2021; Received in revised form 10 April 2022; Accepted 6 June 2022
Available online 10 June 2022

phenomenon can also be seen, using a common expression in protein literature, as a "shift" in the isoelectric point of the protein near the surface, which is no longer equal to that in the bulk. Therefore, what is observed as adsorption on the WSIP can be also interpreted as adsorption on the "correct" side of the isoelectric point of the adsorbed proteins. Theoretical studies have shown that both mechanisms, charge regulation and charge patches, could also act in a cooperative way [17,18]. Remarkably, Lunkad, Barroso and Košovan recently provided a general framework to assess which mechanism should prevail depending on the pH conditions and the specific features of the protein (particularly, the protein charge regulation capacity and its dipolar moment). They used them to explain experiments in the literature where adsorption in the WSIP was observed for different globular proteins [19].

Most of previous studies on the topic have focused on proteins with a fairly rigid structure. This article is devoted to the adsorption of flexible peptides. In this case, the physicochemistry involved in the substrate-protein interaction is not fully understood at the fundamental level for two reasons: (i) the coupling between the chain configurations and the acid/base equilibria of the ionizable groups of the chain and (ii) the complex interaction between the peptide chain and charged surface. In both phenomena, electrostatic interactions play a fundamental role, whose intensity is highly influenced by the pH-value and the salt concentration. In particular, we aim to understand the conditions under which of the two mechanisms, charge patches or charge regulation, predominates.

As a model system, we have chosen the adsorption of casein macropeptide (CMP). CMP is one of the most abundant proteins in the milk whey [20], and it has applications in nutritional management of phenylketonuria, hemagglutination inhibition, prevention of intestinal infection, among others [21], or even in the development of infantile milk formulas [22,23]. Nowadays, the global milk whey production is estimated at 180 million tons per year, implying a global CMP production of roughly 160 thousand tons per year [20]. Without proper treatment, it can have a toxic impact on the environment causing excess oxygen consumption, impermeabilization and/or eutrophication [24]. In this scenario, the development of an efficient method to purify CMP from the milk whey is desirable, a problem which has been approached using different chromatographic techniques and, in particular, ion exchange membranes [25–27].

CMP consists of a relatively short chain with 64 amino acids which, in solution, presents a very flexible structure with a huge number of accessible conformations, and it is often classified as an intrinsically disordered protein (IDP) [28]. Moreover, the conformational states of CMP has been found to be very pH sensitive, suggesting that conformational and ionization degrees of freedom are highly coupled [29]. In addition, CMP is usually present in the glycosylated form. The most common saccharide bound to the protein is N-acetyl neuraminic acid (NeuNAc) [30], a sialic acid which modifies the ionization properties of the peptide, including its isoelectric point (pI).

In this work CMP is modeled using a coarse-grained model. By means of constant-pH Monte Carlo simulations, both conformational and ionization properties are calculated on the same foot. Despite its simplicity, this approach has been successfully applied to polyelectrolytes [16,31–37] and has been recently extended to model peptides and IDPs [38–44]. Remarkably, the obtained results have been found to match ellipsometry [38,39], X-ray scattering [40,41] experiments of IDPs. Moreover, they have been able to quantitatively predict the titration curves of short peptides obtained by nuclear magnetic resonance (NMR), potentiometry and capillary zone electrophoresis [43,44].

The model proposed and simulations are briefly outlined in Section 1. Section 2 The obtained titration curves in absence of charged surface, a situation which is taken as a reference state, is discussed in Section 2. The adsorption onto the charged surface is analyzed in Section 3. Special attention is paid to the conditions under which adsorption in the WSIP is obtained, and which of the mechanisms is the responsible for this behavior: as will be shown, charge regulation for the positively charged substrates and charge patches for the negatively charged surfaces. The discussions extend to both the aglycosilated and the fully glycosylated forms of CMP.

2. Model and simulations

The simulated system consists of one CMP molecule, monovalent salt ions, and a uniformly charged flat surface. The solvent (water) is implicitly modeled as a dielectric continuum.

The primary structure a CMP peptide is shown in Fig. 1. It contains sixteen ionizable residues. Four of them are basic (three lysines and the N-terminal), depicted in blue color. They are not uniformly distributed but placed at one of the ends of the chain, which leads to an asymmetric distribution of positive charges (charge patches) when they are protonated. The rest twelve ionizable groups, represented in red color, are acidic (eight glutamic acids, two aspartic acids, the C-terminus and the phosphorylated group in *Ser44*, denoted *PSer* in the figure). Moreover, CMP can be found in A and B variants, which differ in two aminoacids: variant A contains *Thr31* and *Asp43* while variant B includes *Ile31* and *Ala43*. Here we focus on variant A since our preliminary calculations indicated that this difference does not significantly affect the obtained results. Furthermore, CMP can undergo glycosylation on six residues, *Thr*26, *Thr*28, *Thr*30, *Ser*36 and *Thr*37, marked with asterisks in Fig. 1. In the most common case, the one here considered, only three out of them are glycosylated. Moreover, it has been determined that CMP can bind a maximum of six sialic acid groups (denoted as *Sia*) [21,45]. Among the possible glycosylation states, we have chosen the fully glycosylated CMP, with three sialic acid dimers located at *Thr26*, *Thr30* and *Thr37*, so that they are equidistantly located. As a result, gCMP contains six more acidic groups than aCMP.

In the simulations, the peptide residues and the C/N-terminus are replaced by beads linked by harmonic springs. The resulting coarse grained model results in linear flexible chains, with six pendant acid groups in the case of gCMP. Typical adsorbent molecules used to purify CMP in chromatography experiments are chitosan mini spheres with an adjustable size of around 1 mm. Since the characteristic size of CMP is on the nanometer scale, we can replace the absorbent particle by a flat charged plane. On the other hand, chitosan is a branched polymer that can be functionalized by specific reactions to generate positive or negative surface charge density σ_s [46].

A more detailed description of the model (interaction potentials, beads, and ions size, etc.) is provided as Supplementary Information (SI) in Section S1.

The configurational space is sampled according to a probability proportional to $exp(-\beta E)$ by means of a standard Metropolis algorithm. In each Monte Carlo (MC) step, the following trial movements are attempted: i) translational motion of small ions; ii) translational motion of each bead in the peptide chain; iii) translational and rotational motions of the peptide chain; iv) pivot motion of a segment of peptide chain on a random bead (including the side chains in gCMP case); v) protonate/deprotonate an titratable group, which is coupled to the creation/elimination of one small ion in order to maintain electroneutrality;[47,48] vi) creation/elimination of a neutral pair of small ions, in order to keep the salt concentration constant [49,50]. The trial probabilities of steps i) to vi) are reported as SI (Section S1).

The simulation box has dimensions $W \times W \times L$ with $W = 10\text{nm}$ and $L = 50\text{nm}$. The charged surface is perpendicular to the z-axis, and it is placed at $z = 0$. An auxiliary rigid wall is placed at $z = L$. Periodic boundary conditions are applied in the x and y directions [50,51]. The total number of MC steps is 2×10^6: the first 10^6 steps stabilize the ionization process and the remaining 10^6 steps are used to calculate the ensemble averages.

The average net charge of the peptide is given by $Z_{\text{CMP}} = \sum_1^N \langle q_i \rangle$,

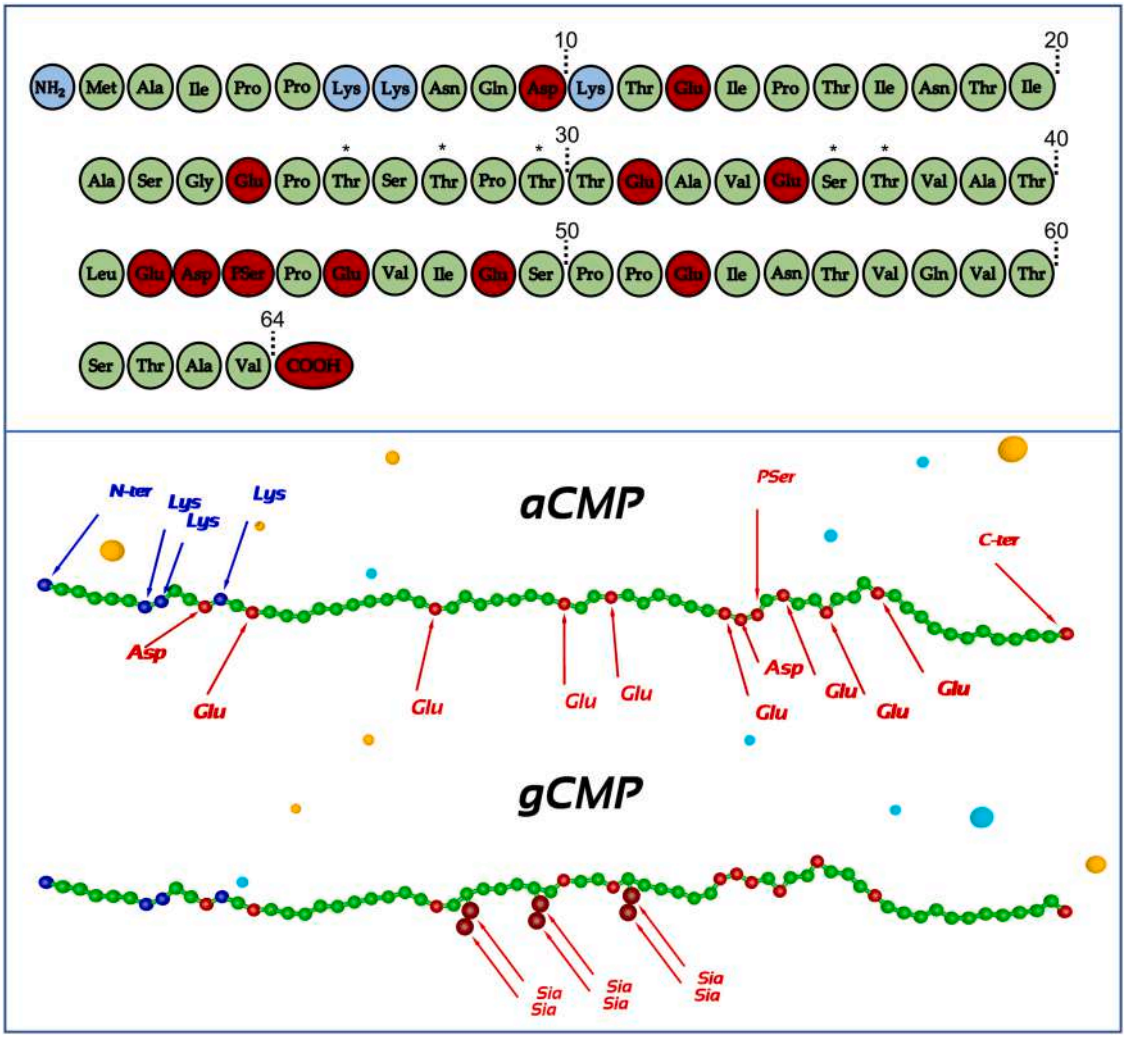

Fig. 1. Upper panel: primary structure of variant A of CMP. The acidic, basic and inert aminoacids are depicted in red, blue and green respectively. Lower panel: scheme showing the bead-and-spring model for aCMP and gCMP. The small cations and anions are colored in cyan and orange, respectively. The chains are shown in their extended form, a rather improbable configuration, only to facilitate the visual identification of the different groups.

where $\langle q_i \rangle$ is the ensemble average charge per group *i*. The concentration profiles $c(z)$ of beads and small ions are calculated by using histograms. The simulation box is divided in M parallel bins of area W^2 and thickness $\Delta z = 0.1$nm, located at positions $z = z_j = j\Delta z$ so that

$$c(z) \approx c(z_j) = \frac{\langle n(z_j) \rangle}{V_b}; \; j = 1, \ldots, \quad M \tag{1}$$

where $\langle n(z_j) \rangle$ is the ensemble average number of particles at a distance z from the surface between z_j and $z_j + \Delta z$, and $V_b = W^2 \Delta z$ is the bin volume. The adsorption coverage of CMP, Γ_{CMP}, is defined as the total number of the protein beads in the volume lying between the surface and a parallel plane located at distance z_{max}

$$\Gamma = \int_0^{z_{max}} c(z)dz \approx \sum_{j=1}^{z_{max}/\Delta z} c(z_j)\Delta z \tag{2}$$

The value $z_{max} \approx 3$nm is somehow arbitrary. We chose this value after considerations about the observed CMP concentration profiles (See Section S3 in the supporting information), which are almost zero for $z > z_{max}$ when CMP is strongly adsorbed onto the surface.

3. Titration behavior of CMP in absence of charged surface

Let us analyze the titration behavior of CMP in the presence of ions but in absence of charged surface, which will be further used as a reference to assess the effect of the charged surface on the macromolecular charge. The net charge Z_{CMP} is shown for aCMP (Fig. 2A) and gCMP) (Fig. 2B) for pH-values ranging from 2 to 7 and added salt concentrations c_{Salt} of 1mM (circles), 10mM (squares) and 100mM (diamonds). In order to evaluate the role of electrostatic interactions, the ideal titration curve (i.e. non-interacting ionized groups, Eqs. S7 and S8 in SI) is also depicted in green color.

aCMP Fig. 2A shows that at low enough pH-values, all the titratable groups of aCMP are protonated, and the net charge reaches the maximum value, $Z_{CMP} = +4$: the four basic groups (three lysine groups and the N-terminus) are positively charged while the acidic groups are neutral. In increasing the pH-value, Z_{CMP} monotonically decreases due to deprotonation of the acidic groups until the isoelectric point is achieved at pH $\approx$ 3.7. Both for positive and negative net charges, deviations from the ideal titration curve are observed due to electrostatic repulsion. This effect is larger for lower salt concentrations, since the electrostatic screening induced by the small ions decreases and the repulsion between ionized groups becomes stronger. Finally, at high enough pH-values the net charge reaches its more negative value $Z_{CMP} = -8$, as expected.

The titration curve of *gCMP* is depicted in Fig. 2B. The isoelectric point is pI $\approx$ 2.5, lower than the one of aCMP, due to the presence of the additional six sialic acid groups ($pK_a = 2.6$). Again, the titration curves clearly deviate from the ideality, especially for pH > 3, for all the salt

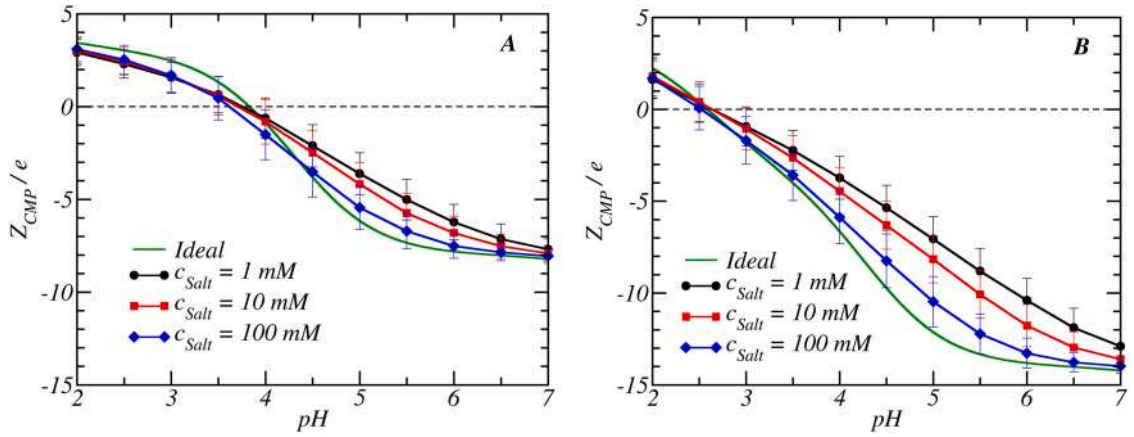

Fig. 2. Net charge Z_{CMP} as a function of the pH-value for aCMP (A) and gCMP (B) at salt concentrations 1 mM (circles), 10 mM (squares) and 100 mM (diamonds). The green line represents the ideal titration curve (non-interacting ionized groups).

concentrations. As expected, these deviations are larger than in the case of *aCMP* due to the higher negative charge density contributed by the extra sialic acid groups.

Despite the simplicity of our model, the obtained isoelectric points of aCMP and gCMP agree reasonably well with the experimental values previously reported in the literature. Kreuβ et al. estimated by electrophoresis the isoelectric point of CMP of 4.1 ± 0.5 (aCMP) and 3.1 ± 0.5 (gCMP) [29]. These values can be contrasted by the theoretical estimation provided by pepKalc [52] and ICP2 [53] online servers, which estimate an isoelectric point of 3.9 and 4.0 ± 0.2 for aCMP, respectively. Unfortunately, these servers cannot estimate the isoelectric point of gCMP since they are not prepared to handle glycosylated aminoacids yet. Our model predicts values of the isoelectric point slightly below the above-mentioned values from other sources. These small deviations could be due to some specific interactions neglected in our model, such as hydrogen bonding or hydrophobic interactions.

The conformational properties of CMP in bulk solution predicted by our model are discussed in detail in the supporting information (Section S2). Remarkably, our model predicts a radius of gyration of 2.0 ± 0.1 nm, (pH = 6.5) which is reasonably in good agreement with the experimentally found hydrodynamic size (2.3 nm at the same pH value), suggesting that our model provides a reasonable approximation of aCMP conformational properties in solution [54].

4. Adsorption of CMP onto a charged substrate

4.1. Adsorption of aCMP

We first focus in the case of aCMP adsorbing into a surface with a surface with negative charge density, $\sigma_S = -0.50\ e/nm^2$. Note that adsorbents with this charge density are experimentally feasible. One example can be found in the work by Galisteo and Norde on the adsorption of lysozyme and α-lactalbumin on poly(styrenesulphonate) latices using two surfaces with charge densities of $-8.1 \pm 0.6\ \mu C/cm^2$ ($\approx -0.50\ e/nm^2$) and $-14.9 \pm 0.7\ \mu C/cm^2$ ($\approx -0.92\ e/nm^2$) [55].

The adsorption coverage Γ as a function of the pH-value in presence of such surface is shown in Fig. 3A. Γ decreases with the salt concentration c_{salt} at pH < pI, when the peptide has a positive net charge (thus at the 'conventional' side of its pI), since the electrostatic attraction between substrate and peptide is screened by the small ions. A snapshot of this situation is shown Fig. 4A, with pH= 2 and c_{salt}= 1 mM. The positive charged residues, in blue color, are attached to the negative surface. Note that because of charge patches, the chain is adsorbed by the positive end while the rest of the chain, which remains neutral, forms loops and other flexible structures. When the salt concentration increases, the accumulation of small cations (cyan) near the surface screens the surface electric field, weakens the surface-peptide attraction, and the adsorption degree decreases. The same conclusion is supported by the profile concentrations, which are provided as SI: maxima in the

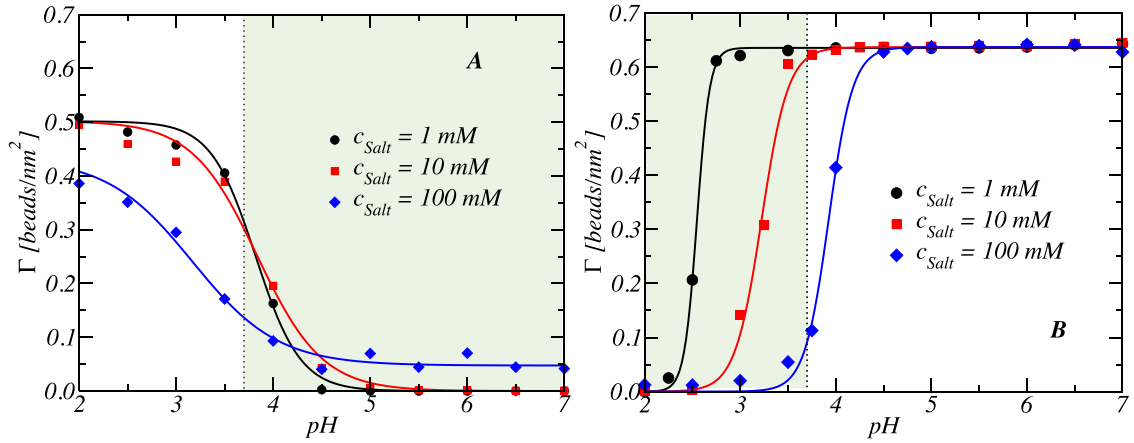

Fig. 3. Adsorption degree of aCMP on a charged substrate as a function of pH at salt concentrations 1 mM (black), 10 mM (red) and 100 mM (blue). A) Negatively charged surface ($\sigma_S = -0.50\ e/nm^2$). B) Positively charged surface ($\sigma_S = 0.50\ e/nm^2$). Vertical dotted line reflects the ideal value of $pI = 3.7$ (Fig. 2A) and separates the wrong side of *pI* (green) from the conventional side (white). The continuous lines are to guide the eye.

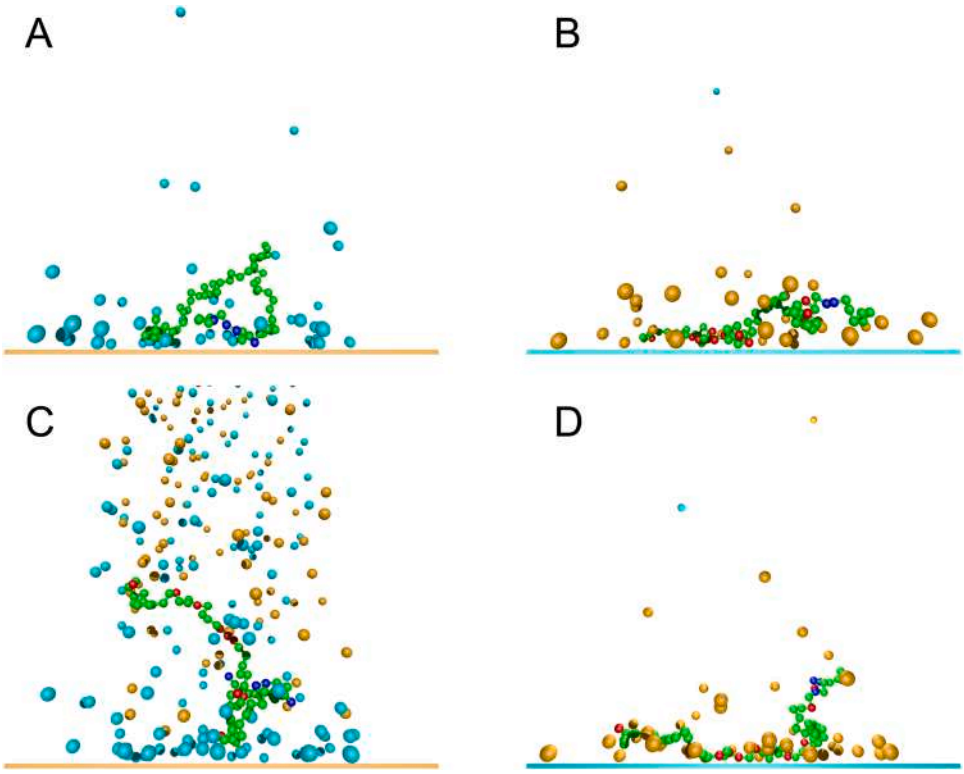

Fig. 4. Snapshots of the Monte Carlo simulation for aCMP adsorbed onto a charged surface. The negatively (positively) charged surface is depicted in orange (cyan) color; small anions (cations) are also shown in orange (cyan) color; neutral, negative and positive bead are represented in green, red and blue, respectively. The surface charge densities are $\sigma_S = -0.5\ e/\text{nm}^2$ for A and C, and $\sigma_S = 0.5\ e/\text{nm}^2$ for B and D. A) pH = 2, c_{Salt} = 1 mM. B) pH = 7, c_{Salt} = 1 mM. C) pH = 5, c_{Salt} = 100 mM. D) pH = 3, c_{Salt} = 1 mM.

concentration of the positive species are observed at $z \sim 0.5$ nm (positively charged residues and small cations) and at $z \sim 1$ nm (beads) are found.

In the same figure (Fig. 3A), some degree of adsorption is observed in the WSIP. This fact is particularly surprising when a plateau with $\Gamma \sim 0.05$ beads / nm^2 is formed at the highest salt concentration c_{salt}= 100 mM for pH> 4.5. Under these conditions, all the acidic groups are negatively charged, as shown in Fig. 2. Moreover, unlike what happens in the 'conventional' side of the isoelectric point, peptide adsorption is promoted at high salt concentrations. This apparently anomalous situation can be understood with the help of the snapshot in Fig. 4C, for pH= 5 and c_{salt}= 100 mM. Due to charge patches, one of the ends of the chain is adsorbed to the surface, although the rest of the peptide is negatively charged. The repulsion between the surface and the negative beads is overcome because of the screening produced by the high salt concentration. Moreover, the negative tail is perpendicular to the surface to minimize repulsion. Therefore, we conclude that charge patches, in combination with electrostatic screening, is the reason for the adsorption in the WSIP when the surface is negatively charged.

The scenario is different for a positively charged substrate ($\sigma_S = +0.50\ \text{e/nm}^2$), as depicted in Fig. 3B. At large enough pH-values, the adsorption coverage increases reaching a plateau with $\Gamma_{max} \sim 0.66$ beads/nm^2. Note that $\Gamma_{max} = 0.66$ beads/nm^2 corresponds to the maximum possible amount of protein adsorbed given that there is only one explicit aCMP chain in the system, which corresponds to a concentration of adsorbed protein of 0.11 mg/m^2. This value is significantly larger than the maximum Γ obtained for negatively charged surfaces, suggesting a stronger adsorption in the case of a positively charge surface. Also note that as the salt concentration decreases, the adsorption profiles and the corresponding plateau is shifted to low pH-values. As a result, significant adsorption in the WSIP is obtained at low c_{salt} values, contrary to the observed behavior for negatively charged substrates, for which adsorption was promoted at high salt concentration. This fact suggests that adsorption in the WSIP cannot be explained only in terms of charge patches.

Snapshots corresponding to adsorption on a positively charged surface are plotted in Fig. 4B (pH=7 and c_{salt}=100 mM) and 4D (pH=3 and c_{salt}=1 mM). In Fig. 4B the chain exhibits conventional adsorption, as expected. The chain contains a dozen negative charges to only three positive charges (the Lysine groups are still protonated). On the other hand, a case of adsorption in the WSIP is depicted in Fig. 4D. In this case, charge regulation produced by the surface induces the deprotonation of the acid groups, which become negatively charged. Both in Fig. 4B and D, the chain is attached to the surface by means of a train-like conformation. A detailed analysis of how the conformational properties of CMP change when adsorbed into the surface is provided in the supporting information (see Section S4).

In order to clarify this point, let us analyze Z_{CMP} as a function of the pH-value in presence of the charged surface, which is shown in Fig. 5A ($\sigma_S = -0.50\ \text{e/nm}^2$) and 5B ($\sigma_S = +0.50\ \text{e/nm}^2$) for the same salt concentrations as in Fig. 2. For the negatively charged surface, the calculated net charge is qualitative different to the one obtained for the isolated peptide. The main difference relies on the fact that in presence of the surface, for pH > pI, Z_{CMP} is lower and closer to the ideal titration curve: peptide-surface electrostatic repulsion promotes the protonation of the acidic groups, which become neutral. For pH < pI, the interaction with the surface is weaker and induces two opposite mechanisms: the negative surface charge tends to charge positively the chain by protonating the basic groups. However, this fact leads to an increase of the repulsion between positive charges in the chain. As a result, the departure of ideality is not monotonic with salt concentration. In short, for $\sigma_S < 0$ the impact of the surface on the ionization properties of the protein is rather modest.

The situation is very different for $\sigma_S > 0$. Comparing Fig. 5B (in presence of surface) and Fig. 2A (isolated peptide), the positively charged substrate dramatically affects the value of Z_{CMP} for the whole range of pH-values, and strong departure from ideality is observed. The presence of the surface induces deprotonation of the acidic groups (see Section S5 in the SI) so that the peptide becomes negatively charged even for pH-values lower than the isoelectric point corresponding to the isolated protein (pI ∼ 3.7). The real isoelectric point is shifted to more acidic pH-values: pI ∼ 3.5, 3 and 2.5 for c_{salt}= 100 mM, 10 mM and

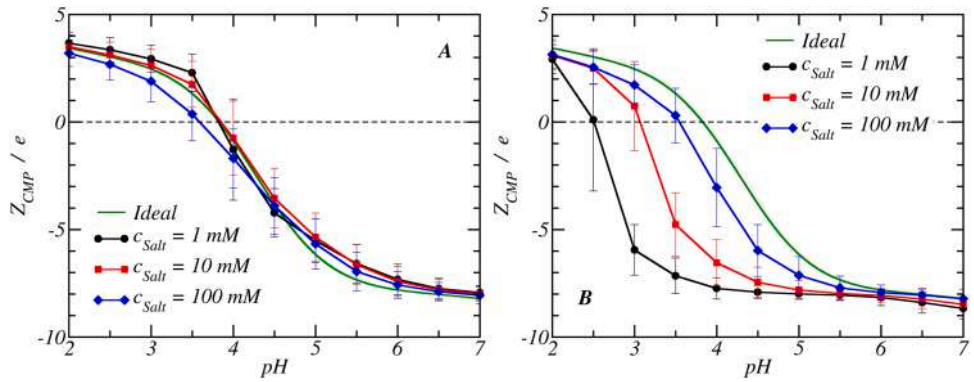

Fig. 5. Net charge of aCMP on a charged substrate as a function of pH at salt concentrations 1 mM (black), 10 mM (red) and 100 mM (blue). A) Negatively charged surface ($\sigma_S = -0.50\,e/nm^2$). B) Positively charged surface ($\sigma_S = 0.50\,e/nm^2$).

1 mM, respectively. Consequently, a much more intense peptide-substrate attraction is produced. This effect is more intense for low salt concentrations and thus lower electrostatic screening, as expected. In summary, for a positively charged surface, the responsible of adsorption in the WSIP is not charge patches, but charge regulation.

4.2. Adsorption of gCMP

As commented above, gCMP differs from aCMP in six extra sialic groups and, as a result, the isoelectric point of *gCMP* is 2.5, lower than the one of aCMP.

The adsorption coverage of gCMP is shown in Fig. 6 for c_{Salt}= 1 mM (black), 10 mM (red) and 100 nM (blue). As a general trend, the effects observed for gCMP coincide with that of aCMP, but shifted to lower pH-values due to the higher negative charge density. In presence of a negatively charged surface, with $\sigma_S = -0.50\ e/nm^2$ (Fig. 6A), significant peptide adsorption is observed for pH < 2.5, for which the chain and the net surface charge have opposite sign. Adsorption decreases with salt concentration since electrostatic screening lower the protein-substrate attraction. For pH > 2.5, charge patches is the responsible of the adsorption in the WSIP. Again, the chain remains adsorbed by the positively charged end at high enough salt concentrations, so that the repulsion between surface and the negative charge of the peptide is screened by the salt ions.

On the other hand, if the surface is positively charged (Fig. 6B), the adsorption coverage reaches its maximum value $\Gamma_{max} \sim 0.72$ beads / nm^2 for pH-values larger than 3.5 and for all the salt concentrations. Moreover, for c_{Salt}= 1 mM, one obtains that $\Gamma \approx \Gamma_{max}$ for the whole range of pH-values, even in the WSIP. For c_{Salt}= 10 mM significant adsorption in the WSIP is also taking place. As in the case of aCMP, calculated net peptide charges indicate that this effect results from charge regulations induced by the surface (see Section S6 in the supporting information).

5. Conclusions

In this work, the adsorption of casein macropeptide (CMP) onto a charged surface has been studied by means of constant-pH Monte Carlo simulations. The substrate has been modeled as a uniformly charged plane while the peptide is represented by a bead-and-spring model. Conformational and protonation equilibria are considered on the same foot. Both the glycosylated (gCMP) and aglycosylated (aCMP) forms of CMP are investigated.

For different reasons, the adsorption on the 'wrong side' of the isoelectric point is observed both for positively and negatively charged surfaces. For a negatively charged surface, the key point is the patchy distribution of positive charges. The protonated basic groups are placed at the end of the chain, which remain attached to the surface, while the repulsive force between the surface and the negative part of the peptide is screened by the added salt. Adsorption is thus favored at high salt concentrations. Moreover, the negatively charged tail adopts a conformation perpendicular to the surface, to minimize the electrostatic repulsion. Therefore, charge patches and electrostatic screening work together to allow the protein to be adsorbed.

Conversely, for a positively charged surface the crucial mechanism for adsorption in the WSIP is charge regulation. The presence of the

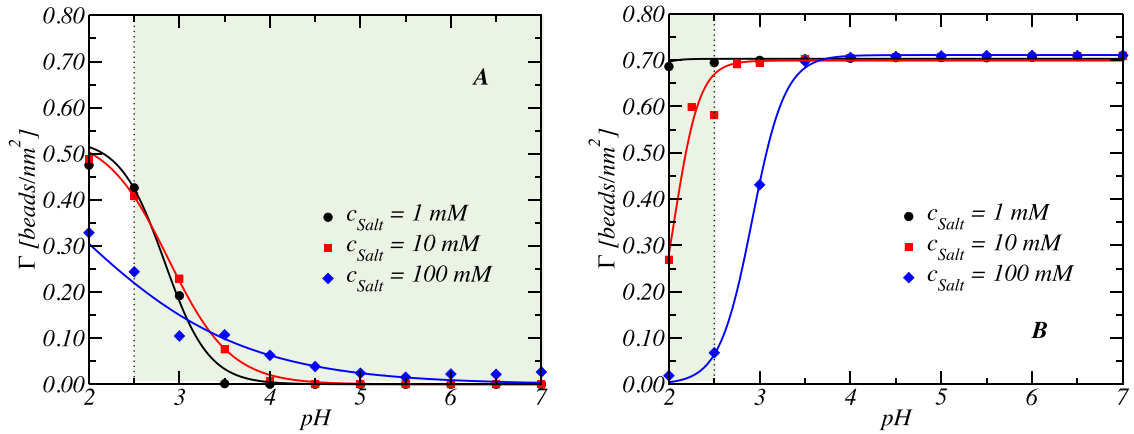

Fig. 6. Adsorbed amount of *gCMP* on a charged substrate as a function of *pH* at added salt concentrations of 1 mM (circles), 10 mM (squares) and 100 mM (diamonds). A) Negatively charged surface ($\sigma_S = -0.50\ e/nm^2$). B) Positively charged surface ($\sigma_S = +0.50\ e/nm^2$). Vertical dotted line reflects the ideal value of *pI* = 2.5 (Fig. 2B) and separates the wrong side of *pI* (green) from the conventional side (white). The continuous lines are to guide the eye.

surface induces dramatic deprotonation of the acidic groups, negatively charging the protein, and generating a net attractive force for the substrate. This effect is enhanced at low salt concentrations. A train-like conformation of the adsorbed peptide is favored.

In summary, our results suggest that aCMP can adsorb in the WSIP due to both mechanisms proposed in the literature, charge regulation and charge patches, in good agreement with the recent observations of Lunkad et al. [19]. In addition, our results show that even in presence of the same protein and similar pH conditions, the mechanism provoking the adsorption in the WSIP can differ depending on the charge of the adsorbent (i.e. the surface). Adsorption in the WSIP is observed both for the aCMP and gCMP forms, although in the latter case it takes place at lower pH-values. Therefore, preferential adsorption is expected for gCMP rather than aCMP at low pH-values.

In conclusion, CMP seems to be a good candidate as a model system to guide and design new experiments on adsorption of flexible proteins onto charged surfaces. Up to our knowledge, the adsorption of CMP in the WSIP has not been experimentally reported yet. According to our results, the optimal conditions for adsorbing CMP in the WSIP are different for a negatively charged adsorbent (low salt concentration) than for a positively charged adsorbent (high salt concentrations). This fact suggests further experiments should be performed to address open questions such as the use of adsorption to separate different forms of the same protein (in our case aCMP and gCMP), the role of multi-valent ions, or the possibility of charge regulation to be experienced by both the surface and the peptide [56].

Declaration of Competing Interest

The authors declare that they have no known competing financial interests or personal relationships that could have appeared to influence the work reported in this paper.

Acknowledgment

The authors are thankful to Dr. Peter Košovan for insightful discussion. Andrea Muñoz is gratefully acknowledged for the manuscript proofreading. M.M.A. and C.F.N. acknowledge the financial support from Universidad Tecnológica Nacional (PIDs PAUTNSR0006583 and PAUTNSR0006584). P.M.B acknowledges the financial support from Czech Science Foundation (project 21-31978J) and from Santander Bank (grant Becas Santander Iberoamérica Investigación España 2019–2020). S.M., J.L.G. and F.M. acknowledge the financial support from Generalitat de Catalunya (Grants 2017SGR1033 and 2017SGR1329). S.M. and F.M. acknowledge Spanish Structures of Excellence María de Maeztu program through (Grant MDM-2017 {0767}). J.L.G. also acknowledges Grant PID2019–107033GB-C21 funded by MCIN/AEI/10.13039/501100011033. M.F.B acknowledges the financial support from the Agencia Nacional de Promoción Científica y Tecnológica de la República Argentina (PICT 2016-0697).

CRediT authorship contribution statement

Pablo M. Blanco: Conceptualization, Methodology, Writing - Original Draft. **Micaela M. Achetoni**: Methodology, Software, **Josep L. Garcés**: Conceptualization, Writing - Review & Editing, **Sergio Madurga**: Conceptualization, Writing - Review & Editing, **Francesc Mas**: Conceptualization, Writing - Review & Editing, **María F. Baieli**: Writing - Review & Editing, **Claudio F. Narambuena**: Conceptualization, Writing - Original Draft, Supervision, Funding acquisition.

Appendix A. Supporting information

Supplementary data associated with this article can be found in the online version at doi:10.1016/j.colsurfb.2022.112617.

References

[1] W. Senaratne, L. Andruzzi, C.K. Ober, Self-assembled monolayers and polymer brushes in biotechnology: current applications and future perspectives, Biomacromolecules 6 (2005) 2427–2448.
[2] T. Hattori, R. Hallberg, P.L. Dubin, Roles of electrostatic interaction and polymer structure in the binding of β-lactoglobulin to anionic polyelectrolytes: measurement of binding constants by frontal analysis continuous capillary electrophoresis, Langmuir 16 (2000) 9738–9743.
[3] R. de Vries, F. Weinbreck, C.G. de Kruif, Theory of polyelectrolyte adsorption on heterogeneously charged surfaces applied to soluble protein–polyelectrolyte complexes, J. Chem. Phys. 118 (2003) 4649–4659.
[4] C.G. De Kruif, F. Weinbreck, R. De Vries, Complex coacervation of proteins and anionic polysaccharides, Curr. Opin. Colloid Interface Sci. 9 (2004) 340–349.
[5] A. Wittemann, M. Ballauff, Interaction of proteins with linear polyelectrolytes and spherical polyelectrolyte brushes in aqueous solution, Phys. Chem. Chem. Phys. 8 (2006) 5269–5275.
[6] D. Srivastava, E. Santiso, K. Gubbins, F. Luís Barroso da Silva, Computationally mapping pKa shifts due to the presence of a polyelectrolyte chain around whey proteins, Langmuir 33 (2017) 11417–11428.
[7] K. W. Mattison, P. L. Dubin, I. J. Brittain, Complex formation between bovine serum albumin and strong polyelectrolytes: effect of polymer charge density, J. Phys. Chem. B 102 (1998) 3830–3836.
[8] C.G. De Kruif, F. Weinbreck, R. De Vries, Complex coacervation of proteins and anionic polysaccharides, Curr. Opin. Colloid Interface Sci. 9 (2004) 340–349.
[9] Y. Xu, M. Mazzawi, K. Chen, L. Sun, P.L. Dubin, Protein purification by polyelectrolyte coacervation: influence of protein charge anisotropy on selectivity, Biomacromolecules 12 (2011) 1512–1522.
[10] C. Yigit, J. Heyda, M. Ballauff, J. Dzubiella, Like-charged protein-polyelectrolyte complexation driven by charge patches, J. Chem. Phys. 143 (2015) 64905.
[11] A. Lošdorfer Božič, R. Podgornik, pH dependence of charge multipole moments in proteins, Biophys. J. 113 (2017) 1454–1465.
[12] J.G. Kirkwood, J.B. Shumaker, Forces between protein molecules in solution arising from fluctuations in proton charge and configuration, Proc. Natl. Acad. Sci. USA 38 (1952) 863–871.
[13] M. Lund, B. Jönsson, Charge regulation in biomolecular solution, Q. Rev. Biophys. 46 (2013) 265–281.
[14] F. Luís Barroso da Silva, M. Lund, B. Jönsson, T. Åkesson, On the complexation of proteins and polyelectrolytes, J. Phys. Chem. B 110 (2006) 4459–4464.
[15] F. Luís Barroso da Silva, M. Boström, C. Persson, Effect of charge regulation and ion–dipole interactions on the selectivity of protein–nanoparticle binding, Langmuir 30 (2014) 4078–4083.
[16] P.B. Torres, E. Quiroga, A.J. Ramirez-Pastor, V. Boeris, C.F. Narambuena, Interaction between β-lactoglobuline and weak polyelectrolyte chains: a study using Monte Carlo simulation, J. Phys. Chem. B (2019), https://doi.org/10.1021/acs.jpcb.9b03276.
[17] W.M. de Vos, F.A.M. Leermakers, A. de Keizer, M.A. Cohen Stuart, J. Mieke Kleijn, Field theoretical analysis of driving forces for the uptake of proteins by like-charged polyelectrolyte brushes: effects of charge regulation and patchiness, Langmuir 26 (2009) 249–259.
[18] F.M. Boubeta, G.J.A.A. Soler-Illia, M. Tagliazucchi, Electrostatically driven protein adsorption: charge patches versus charge regulation, Langmuir 34 (2018) 15727–15738.
[19] R. Lunkad, F.L. Barroso da Silva, P. Košovan, Both charge-regulation and charge-patch distribution can drive adsorption on the wrong side of the isoelectric point, J. Am. Chem. Soc. 144 (1813–1825) (2022).
[20] C. Baldasso, T.C. Barros, I.C. Tessaro, Concentration and purification of whey proteins by ultrafiltration, Desalination 278 (2011) 381–386.
[21] Neelima, R. Sharma, Y.S. Rajput, B. Mann, Chemical and functional properties of glycomacropeptide (GMP) and its role in the detection of cheese whey adulteration in milk: a review, Dairy Sci. Technol. 93 (2013) 21–43.
[22] T. Nakano, N. Ikawa, L. Ozimek, Use of epichlorohydrin-treated chitosan resin as an adsorbent to isolate κ-casein glycomacropeptide from sweet whey, J. Agric. Food Chem. 52 (2004) 7555–7560.
[23] C. Thomä-Worringer, J. Sørensen, R. López-Fandiño, Health effects and technological features of caseinomacropeptide, Int. Dairy J. 16 (2006) 1324–1333.
[24] M. Aider, D. de Halleux, I. Melnikova, Skim acidic milk whey cryoconcentration and assessment of its functional properties: impact of processing conditions, Innov. Food Sci. Emerg. Technol. 10 (2009) 334–341.
[25] T. Nakano, L. Ozimek, Purification of glycomacropeptide from dialyzed and non-dialyzed sweet whey by anion-exchange chromatography at different pH values, Biotechnol. Lett. 22 (2000) 1081–1086.
[26] S. Doultani, K.N. Turhan, M.R. Etzel, Whey protein isolate and glyco-macropeptide recovery from whey using ion exchange chromatography, J. Food Sci. 68 (2003) 1389–1395.
[27] M.F. Baieli, et al., Affinity chromatography matrices for depletion and purification of casein glycomacropeptide from bovine whey, Biotechnol. Prog. (2017), https://doi.org/10.1002/btpr.2404.
[28] F.-X. Theillet, et al., Physicochemical properties of cells and their effects on intrinsically disordered proteins (IDPs), Chem. Rev. 114 (2014) 6661–6714.
[29] M. Kreuß, T. Strixner, U. Kulozik, The effect of glycosylation on the interfacial properties of bovine caseinomacropeptide, Food Hydrocoll. 23 (2009) 1818–1826.
[30] J. Salcedo, et al., Comparison of spectrophotometric and HPLC methods for determining sialic acid in infant formulas, Food Chem. 127 (2011) 1905–1910.

[31] C.F. Narambuena, E.P.M. Leiva, E. Pérez, Counterion condensation on polyelectrolyte chains adsorbed on charged surfaces, Colloids Surf. A Physicochem. Eng. Asp. 487 (2015).
[32] P. Torres, et al., Protonation of β-lactoglobulin in the presence of strong polyelectrolyte chains: a study using Monte Carlo simulation, Colloids Surf. B Biointerfaces 160 (2017).
[33] M. Stornes, P. Linse, R. S. Dias, Monte Carlo simulations of complexation between weak polyelectrolytes and a charged nanoparticle. Influence of polyelectrolyte chain length and concentration, Macromolecules 50 (2017) 5978–5988.
[34] P. Blanco, S. Madurga, F. Mas, J. Garcés, Coupling of charge regulation and conformational equilibria in linear weak polyelectrolytes: treatment of long-range interactions via effective short-ranged and pH-dependent interaction parameters, Polymers 10 (2018) 811.
[35] M. Stornes, B. Shrestha, R.S. Dias, pH-dependent polyelectrolyte bridging of charged nanoparticles, J. Phys. Chem. B 122 (2018) 10237–10246.
[36] P.M.B. Andrés, S. Madurga, C. Narambuena, F. Mas, J.L. Garcés, Role of charge regulation and fluctuations in the conformational and mechanical properties of weak flexible polyelectrolytes, Polymers (2019), https://doi.org/10.3390/polym11121962.
[37] P.M. Blanco, S. Madurga, F. Mas, J.L. Garcés, Effect of charge regulation and conformational equilibria in the stretching properties of weak polyelectrolytes, Macromolecules 52 (2019) 8017–8031.
[38] K. Hyltegren, T. Nylander, M. Lund, M. Skepö, Adsorption of the intrinsically disordered saliva protein histatin 5 to silica surfaces. A Monte Carlo simulation and ellipsometry study, J. Colloid Interface Sci. 467 (2016) 280–290.
[39] K. Hyltegren, M. Skepö, Adsorption of polyelectrolyte-like proteins to silica surfaces and the impact of pH on the response to ionic strength. A Monte Carlo simulation and ellipsometry study, J. Colloid Interface Sci. 494 (2017) 266–273.
[40] C. Cragnell, E. Rieloff, M. Skepö, Utilizing coarse-grained modeling and Monte Carlo simulations to evaluate the conformational ensemble of intrinsically disordered proteins and regions, J. Mol. Biol. 430 (2018) 2478–2492.
[41] E. Fagerberg, S. Lenton, M. Skepö, Evaluating models of varying complexity of crowded intrinsically disordered protein solutions against SAXS, J. Chem. Theory Comput. 15 (2019) 6968–6983.
[42] P.M. Blanco, S. Madurga, J.L. Garcés, F. Mas, R.S. Dias, Influence of macromolecular crowding on the charge regulation of intrinsically disordered proteins, Soft Matter 17 (2021) 655–669.
[43] R. Lunkad, et al., Quantitative prediction of charge regulation in oligopeptides, Mol. Syst. Des. Eng. 6 (2021) 122–131.
[44] Lunkad, R., Murmiliuk, A., Tošner, Z., Štěpánek, M. & Košovan, P. Role of pK A in Charge Regulation and Conformation of Various Peptide Sequences, 2021 doi: 10.3390/polym13020214.
[45] D. Mollé, J. Léonil, Heterogeneity of the bovine κ-casein caseinomacropeptide, resolved by liquid chromatography on-line with electrospray ionization mass spectrometry, J. Chromatogr. A 708 (1995) 223–230.
[46] S. Pokhrel, P.N. Yadav, Functionalization of chitosan polymer and their applications, J. Macromol. Sci. Part A 56 (2019) 450–475.
[47] M. Ullner, B. Jönsson, A Monte Carlo study of titrating polyelectrolytes in the presence of salt, Macromolecules 29 (1996) 6645–6655.
[48] T. Kesvatera, B. Jönsson, E. Thulin, S. Linse, Measurement and modelling of sequence-specific pKa values of lysine residues in calbindin D9k, J. Mol. Biol. 259 (1996) 828–839.
[49] J.P. Valleau, L.K. Cohen, Primitive model electrolytes. I. Grand canonical Monte Carlo computations, J. Chem. Phys. 72 (1980) 5935–5941.
[50] G.M. Torrie, J.P. Valleau, Electrical double layers. I. Monte Carlo study of a uniformly charged surface, J. Chem. Phys. 73 (1980) 5807–5816.
[51] D. Boda, K.-Y. Chan, D. Henderson, Monte Carlo simulation of an ion-dipole mixture as a model of an electrical double layer, J. Chem. Phys. 109 (1998) 7362–7371.
[52] K. Tamiola, R.M. Scheek, P. van der Meulen, F.A.A. Mulder, pepKalc: scalable and comprehensive calculation of electrostatic interactions in random coil polypeptides, Bioinformatics 34 (2018) 2053–2060.
[53] L.P. Kozlowski, IPC 2.0: prediction of isoelectric point and pKa dissociation constants, Nucleic Acids Res. 49 (2021) W285–W292.
[54] M.E. Farías, M.J. Martinez, A.M.R. Pilosof, Casein glycomacropeptide pH-dependent self-assembly and cold gelation, Int. Dairy J. 20 (2010) 79–88.
[55] F. Galisteo, W. Norde, Adsorption of lysozyme and α-lactalbumin on poly (styrenesulphonate) latices 1. Adsorption and desorption behaviour, Colloids Surf. B Biointerfaces 4 (1995) 375–387.
[56] M. Stornes, P.M. Blanco, R.S. Dias, Polyelectrolyte-nanoparticle mutual charge regulation and its influence on their complexation, Colloids Surf. A Physicochem. Eng. Asp. 628 (2021), 127258.